Title	Enhancing the mechanical properties of superhydrophobic atmospheric pressure plasma deposited siloxane coatings
Authors(s)	Nwankire, Charles E., Favaro, Gregory, Duong, Quynh-Huong, Dowling, Denis P.
Publication date	2011-01-12
Publication information	Nwankire, Charles E., Gregory Favaro, Quynh-Huong Duong, and Denis P. Dowling. "Enhancing the Mechanical Properties of Superhydrophobic Atmospheric Pressure Plasma Deposited Siloxane Coatings." Wiley, January 12, 2011. https://doi.org/10.1002/ppap.201000069.
Publisher	Wiley
Item record/more information	http://hdl.handle.net/10197/5266
Publisher's statement	This is the author's version of the following article: Nwankire, C. E., Favaro, G., Duong, Q.-H. and Dowling, D. P. (2011), Enhancing the Mechanical Properties of Superhydrophobic Atmospheric Pressure Plasma Deposited Siloxane Coatings. Plasma Processes Polym., 8: 305–315 which has been published in final form at http://dx.doi.org/10.1002/ppap.201000069
Publisher's version (DOI)	10.1002/ppap.201000069

Enhancing the mechanical properties of superhydrophobic atmospheric pressure plasma deposited siloxane coatings

Charles E. Nwankire[1], Gregory Favaro[2], Quynh-Huong Duong[2] and Denis P. Dowling[1]*
denis.dowling@ucd.ie

[1]School of Electrical Electronic and Mechanical Engineering, University College Dublin, Ireland.
[2]CSM Instruments SA, Peseux, Switzerland

Abstract

Surfaces with water contact angles above 150° are regarded as superhydrophobic. In this study the use of atmospheric pressure plasma jet system called PlasmaStream™ to deposit superhydrophobic coatings is investigated. The coatings were deposited from the following liquid precursors: HMDSO, tetramethyl cyclotetrasiloxane (Tomcats) and a mixture of Tomcats and fluorosiloxane. The objective of the study is to investigate how precursor type and deposition conditions, influences the morphology and mechanical performance of the deposited superhydrophobic coatings. Optical profilometry, AFM, SEM, Ellipsometry, XPS, Water contact angle and FTIR techniques were used to evaluate the surface roughness, morphology, thickness and chemical functionality of the deposited coatings. The mechanical properties were evaluated using the Nano Tribometer, Nano Scratch, Ultra Nanoindentation and ultrasonic abrasion tests. Superhydrophobic coatings deposited from a precursor mixture of Tomcats and fluorosiloxane yielded a substantial enhancement in coating adhesion and mechanical durability compared to the superhydrophobic coatings obtained with either Tomcats or HMDSO precursors alone. All three coatings exhibited a 'needle-like' morphology, however in the case of the coating deposited from the precursor mixture, a reduction in the heights of the 'needle' peaks (reduced roughness), combined with an increased level of cross-linking may explain the enhanced mechanical durability of this superhydrophobic coating.

Keywords: superhydrophobic, oleophilic, fluorosiloxane, Nano Scratch, Nanoindentation, mechanical durability.

Introduction

Surfaces with water contact angles greater than 150° are generally regarded as superhydrophobic [1]. There is considerable interest in these surfaces due to their anti-wetting and self-cleaning properties. The superhydrophobic (SH) properties have been reported to depend on both their chemical composition and surface morphology.[1-3] In a review, Genzer et al[2] showed that superhydrophobic surfaces can be achieved by tailoring the chemical composition and physical appearance of surfaces. Lee et al[1] achieved SH surface by grafting polyacrylic acid chains onto nylon surfaces with high surface roughness. Oner et al[3] prepared ultrahydrophobic surfaces by photolithography and hydrophobised using silane reagents. The surfaces were termed ultrahydrophobic because they exhibited advancing and receding water contact angles above 170°.

Some of the other techniques that have been used to fabricate superhydrophobic surfaces include wax solidification,[4] lithography,[3] carbon nano tube alignment by plasma enhanced chemical vapour deposition,[5] polymer reconformation,[6] sol gel,[7] and electrochemical processing.[8] Atmospheric pressure plasmas have also been used and their advantage is firstly the relative speed of superhydrophobic coating deposition and generally only a single step deposition process is required.[9-12] Amongst the precursors used to deposit these atmospheric plasma deposited coatings have been fluorocarbon gases,[12] hexamethyldisilazane[10] and hexamethyldisiloxane (HMDSO).[9, 13] In a previous study involving the PlasmaStream™ atmospheric plasma jet deposition system at UCD, a SH coating was deposited from HMDSO.[9] The superhydrophobicity of the HMDSO coating depended on a relatively fragile needle-like morphology. It has previously been reported that the mechanical durability of SH coatings deposited by plasma fluorination of polybutadiene films was enhanced 8-fold after thermal treatment at 155°C for 1 hr.[14] The objective of this study is to evaluate if the mechanical durability of the superhydrophobic coatings can be enhanced by altering the siloxane precursor chemistry used in the deposition of the SH coatings. In addition to HMDSO, the liquid siloxane precursors investigated were perfluorooctyl triethoxysilane (fluorosiloxane), tetramethyl cyclotetrasiloxane (Tomcats) and a mixture of Tomcats and fluorosiloxane. The ability of any of these precursors to form superhydrophobic coatings has not been reported previously.

Experimental Details

Equipment and materials

The siloxane coatings were deposited onto one-side polished P-type silicon wafers (450 μm thick). These substrates were ultrasonically cleaned in acetone and methanol for 10 minutes respectively and dried in air. Coatings were deposited using the Dow Corning atmospheric pressure plasma jet system called PlasmaStream™, which has been reported in details elsewhere.[15, 16] The system was configured with a dielectric head housing two pin electrodes either side of a pneumatic nebuliser (Burgener Ari Mist nebuliser), through which an aerosol of the precursor was introduced. The resultant helium – aerosol mix exited the system through a 75 mm long x 16 mm diameter dielectric tube. Low frequency electrical power was delivered to both electrodes from a modified PTI 100W rf power supply at a frequency of approximately 5-25 kHz. The entire plasma device was moved over the surface of the substrate in a raster pattern (xy directional scan) using a CNC device with a line speed of 10 mm/second and a step interval of 2.5 mm over the area of 100 x 100 mm. The substrate to source distance (gap distance) was varied from 2 to 8 mm.

Coatings were deposited using the following precursors hexamethyldisiloxane (HMDSO) ($(CH_3)_3SiOSi(CH_3)_3$) (Aldrich 98.5%), tetramethyl cyclotetrasiloxane (Tomcats) ($(HSiCH_3O)_4$) (Aldrich 99%), perfluorooctyl triethoxysilane (fluorosiloxane) ($C_{14}H_{19}F_{13}O_3Si$) (Aldrich 98%) and a mixture of fluorosiloxane and Tomcats. The flow rates investigated for these liquid precursors were in the range 3 to 8 μl/min. Helium (He) gas flow rate was kept constant at 5 μl/min. N_2 gas (flow rate of 100 ml/min) was added to the helium plasma to help reduce the formation of particulates.[17]

Coating contact angle measurements were carried out six days after deposition in order to avoid any effects due to hydrophobic recovery.[16] Coating contact angles were measured at room temperature using a video capture apparatus OCA 20 from Dataphysics Instruments. Deionised water, diiodomethane and ethylene glycol were used as test liquids. Contact angles were measured at three different locations on the coating surface and averaged. The OWRK (Owens, Wendt, Rabel and Kaelbe) method was used to determine the surface energy of the deposited coatings from the contact angle measurements.[18]

Fourier transform infrared spectroscopy (FTIR) measurements were carried out using a Bruker Vertex – 70 system, and the transmission spectra were collected in the range of 400 – 4000 cm^{-1} using a spectral resolution of 4 cm^{-1} after 64 scans.

X-ray photoelectron spectroscopy (XPS) was performed using a Kratos Analytical Axis Ultra photoelectron spectrometer. The instrument has a spherical mirror analyzer with an integrated automatic charge neutralizer and a magnetic lens. A monochromated (Al $K\alpha$) x-ray source was used to record spectra at normal emission.

Surface roughness and morphology analyses of the coating was examined using a Wyko NT1100 optical profilometer scanning at least 3 different areas of 45 x 59 µm in vertical scanning interferometer (VSI) mode, unless stated otherwise in the text. The reported average (*Ra*) and root mean square (*Rq*) surface roughness is the mean of three measurements on different areas of each sample taken in order to verify surface homogeneity. Surface morphology examination was also carried out using a CP-II (Veeco) Atomic Force Microscope (AFM) scanner in non contact mode and a TM-1000 Hitachi TableTOP scanning electron microscope (SEM). The coating thickness and optical properties were measured with the J.A. Woollam M2000 variable angle ellipsometer. Coating thickness was obtained by using multiple angle measurements (65°, 70° and 75°) over a wavelength of 250 to 1690 nm. The refractive index was measured at the wavelength of 632.8 nm.

The mechanical properties of the coatings were evaluated with the CSM Nano Scratch Tester, Nano Tribometer and Ultra Nanoindentation Testers (CSM Instruments, Switzerland).[19]

The Nano Scratch Test was carried out using a 90° sphero-conical stylus with an indenter radius of 10 µm. Three scratches were obtained from each test surface, with an initial scanning load of 0.3 mN and final loads of 40 mN (for Tomcats and HMDSO coatings) and 80 mN (for TCFS coating). The critical loads were determined from the recorded normal force vs. penetration depth curves along the scratch; the respective images have also been taken.

The Nano Tribometer system was used to determine the friction coefficient of the coatings. Loads in the range of 0.05 mN to 1 N were used. A 4 mm diameter 100 Cr6 steel ball (mounted on a stiff lever) was loaded onto the coated samples with a normal force of 0.5 mN. This was moved against the coated samples at a linear speed of 1 cm s^{-1}, and was stopped after 500 laps. The friction coefficient was determined by measuring the deflection force on the cantilevers.

Mechanical properties of the coatings such as Hardness and Elastic Modulus were obtained using an Ultra Nanoindentation Tester equipped with a Berkovich diamond indenter tip.[20] The maximum loading/unloading rate was 40 and 200 µN min^{-1}, while the maximum load was 20 and 100 µN for the coated and uncoated samples respectively. The system was used to measure hardness, H (resistance to local deformation) and elastic modulus, E of the coatings. The latter was estimated by analysing the load-displacement curves based on the Oliver – Pharr method.[21] The resistance of the coatings to plastic deformation (H^3/E^2) and E to H ratio were obtained.[22]

Abrasion resistance is an important parameter in the evaluation of the wear resistance of the coatings. Xiu et al.[23] evaluated the abrasion resistance of superhydrophobic surfaces formed on silicon wafer by potassium hydroxide and metal assisted etching, using a 'Technicloth' wipe as the abrasion surface. It was reported that the superhydrophobic surfaces lost their self-cleaning ability after the abrasion tests. To our knowledge an abrasion resistance test has not been reported previously for use with nm thick coatings. A comparative laboratory test is therefore proposed as part of this study. The test involves immersion of the silicon wafer coated substrates in a 300 ml beaker containing a mixture of 50 wt% deionised water with 20 µm diameter precision micro-abrasive silicon carbide (SiC) particles (Comco Inc, USA). The volume of the aqueous mixture was fixed at 200 cm^3 and into this mixture a UP200H ultrasonic processor probe (Hielscher Ultrasonics GmbH, Germany) was lowered to a distance of approximately 5 mm above the base of the beaker. The height of the ultrasonic probe was maintained at this distance in order to stop the abrasive particles from settling at the bottom of the beaker, thus maintaining uniform sample abrasion. This 200 W, 24 kHz frequency ultrasonic probe operated at a 100% pulse cycle rate and 50% amplitude was housed in a SB3-16 sound protection box. After abrasion with the SiC particles for periods of between 1 and 150 minutes, the test samples were removed, washed with deionised water, followed by air drying. Any remaining abrasive particles on the tested surface were removed using compressed air. The adhesion and abrasion resistance of the tested coatings were evaluated using FTIR and water contact angle measurements. Each test was carried out in triplicate and once the coating had been removed after a given time period and tested, it was re-inserted in the test apparatus for the longer term assessment of abrasion resistance. The results of this 'in-house' abrasion test were correlated with other mechanical test results obtained using Nano scratch, Nano Tribometer and Ultra Nanoindentation equipment (CSM Instruments).

Results and Discussion

HMDSO superhydrophobic coating

The HMDSO coatings were deposited at a precursor flow rate of 3 µl min^{-1} and a gap distance of 8 mm. These parameters were previously established as producing superhydrophobic coatings using the PlasmaStream™ system.[9] The optical profilometry image of a typical HMDSO coating deposited using these deposition conditions is given in Figure 1. This image demonstrates that the coating exhibits a nano-textured 'needle-like' morphology. The water droplet with contact angle measured as 156° is also shown in this figure. Coating surface energy is 5 mN m^{-1}, while the *Ra* and *Rq* are 20 and 26 nm respectively. The coating thickness obtained with ellipsometry was approximately 350 nm. The needle-like coating morphology is most likely due to precursor fragmentation and gaseous phase reactions in the plasma.[17]

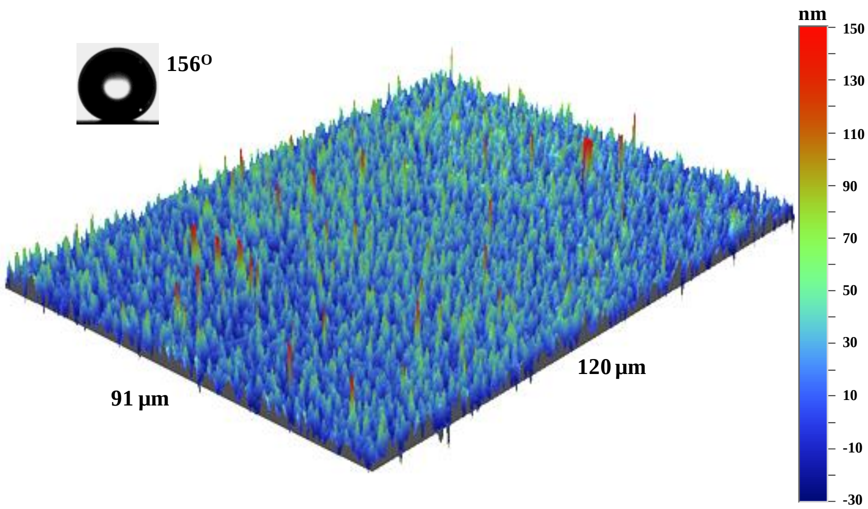

Figure 1: Optical profilometry image of a superhydrophobic HMDSO coating showing the needle-like morphology and water contact angle on the coated surface

Tomcats coating

A series of experiments were carried out to investigate the influence of deposition conditions on the properties of coatings deposited using the Tomcats precursor. Amongst the parameters varied were plasma power, number of passes of the jet over the substrate and gap distance. These coatings were deposited at a precursor flow rate of 5 µl min^{-1}. Table 1 shows the range of plasma deposition parameters investigated.

Table 1: Plasma deposition parameters investigated for the deposition of Tomcats coatings

Plasma power, W	No. of Passes	Gap distance (mm)
3.7 – 7.6	1 – 10	2 – 8

Effect of power - It was observed that with an increase in plasma power there was an increase in surface roughness, thickness and water contact angle. The *Ra* increased from 3 to 19 nm and *Rq* from 4 to 26 nm. The thickness increased from 18 to 694 nm, while the water contact angle increased from 103 to 105°. A possible explanation for these observations is that at low powers (3.7 W), the plasma power is insufficient to achieve complete polymerisation.[15] Thus fragmenting only weak bonds, however at higher powers (7.6 W) multiple bond fragmentation including ring opening reactions will occur leading to the deposition of organosiloxane coatings with high water contact angle, higher thickness and surface roughness.

Effect of number of passes – With the increase of the number of passes of the jet across the wafer surface, coating thickness will increase. In this study from 1 to 10 passes, the thickness increased from 18 to 694 nm. The roughness of the coating deposited after a single pass (*Ra* 3 nm) was similar to that of the uncoated wafer (*Ra* 2 nm), however after 10 passes the *Ra* increased to 19 nm. The corresponding change in water contact angle was from 103 to 155°, while the surface energy decreased from 21 to 5 mN m^{-1}. The decrease in surface energy of atmospheric plasma deposited coatings as precursor flow rate increased has been reported previously by Twomey et al.[24] In this study, although the total surface energy decreased from 21 to 5 mN m^{-1} after 10 passes, the polar surface energy component remained almost constant at approximately 1 mN m^{-1}. The dispersive surface energy component however decreased significantly from 20 to 4 mN m^{-1}. This may indicate that the decreased polarity of the Si-C bond over the Si-O bond influenced the organic content and thus the surface energy of the coatings.[24] The morphology of the deposited Tomcats coating obtained by AFM after a single deposition pass is shown in Figure 2. The coating exhibits both micro and nano rough morphology which has been reported previously to be important for superhydrophobicity.[1-3] The *Ra* value of 12 nm is the mean of three different scans. It was not possible to obtain the surface roughness of the coating deposited after 10 passes using AFM due to the very high coating surface roughness.

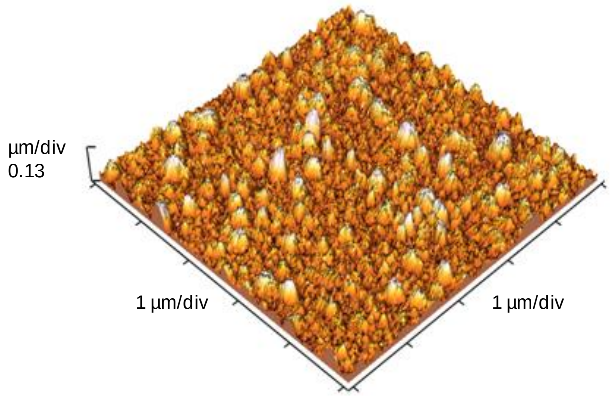

Figure 2: AFM image of Tomcats coating *Ra* 12 nm demonstrating the micro and nano rough morphology

Effect of gap distance - The effect of the gap distance between the jet orifice and the substrate was also examined. As the gap distance was increased from 2 to 8 mm, the water contact angle for the deposited Tomcats coatings decreased from 155° to 90° (Figure 3). There was a corresponding increase in surface energy from 5 to 24 mN/m and the surface roughness (*Ra)* increased from 19 to 152 nm. This result is the opposite to what was observed in the case of the study detailed earlier in which as the coating thickness increased with number of passes, the surface roughness increase and associated with this there was an increase in water contact angle. In this gap distance study a decrease in water contact angle is observed, despite the increase in deposited coating roughness at the higher gap distance. An explanation of this effect is an increase in coating oxidation with gap distance due to a higher level of air permeation into the helium plasma. This conclusion is supported by the work previously carried out by O'Neill et al.[25] They reported that enhanced coating oxidation at the higher gap distance could be attributed to the fluid dynamics of the atmospheric plasma jet system; as the flow of gas exiting the PlasmaStream™ can entrain air which would subsequently oxidize the precursor as it travels towards the substrate.

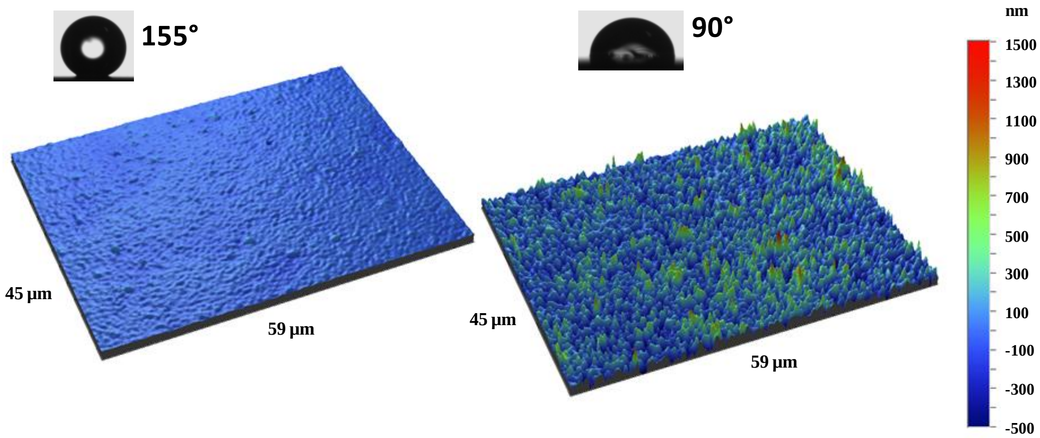

Figure 3: Optical profilometry images showing the morphology of Tomcats coatings at the gap distance of 2 mm (left) *Ra* 19 nm and 8 mm (right) *Ra* 152 nm respectively. Note the decrease in water contact angle for the latter coating.

The FTIR spectra of the Tomcats precursor monomer and plasma polymerised coatings deposited at the gap distance of 2 and 8 mm are given in Figure 4. These spectra confirm retention of the monomer chemistry in the plasma polymerised coatings as previously reported for other plasma deposited coatings.[16] The peak at 1255 cm^{-1} is assigned to the Si-CH_3 functional group (CH_3 symmetric deformation). The Si-C stretching is observed at 760 cm^{-1} and the peaks at 2170 and 890 cm^{-1} are attributed to the absorption and bending frequencies of Si-H group. The asymmetric stretching of the Si-O-Si group is absorbed at 1100 cm^{-1}. The 2970 cm^{-1} band is due to the absorption of the Si-O-CH_3 functional group.[26] The broad peak at 3300 cm^{-1} which is attributed to Si-OH group is almost absent in the case of the 2 mm gap distance but is relatively intense in the spectrum of the coating deposited at the 8 mm gap distance. This confirms the higher level of oxidation of the latter coating.

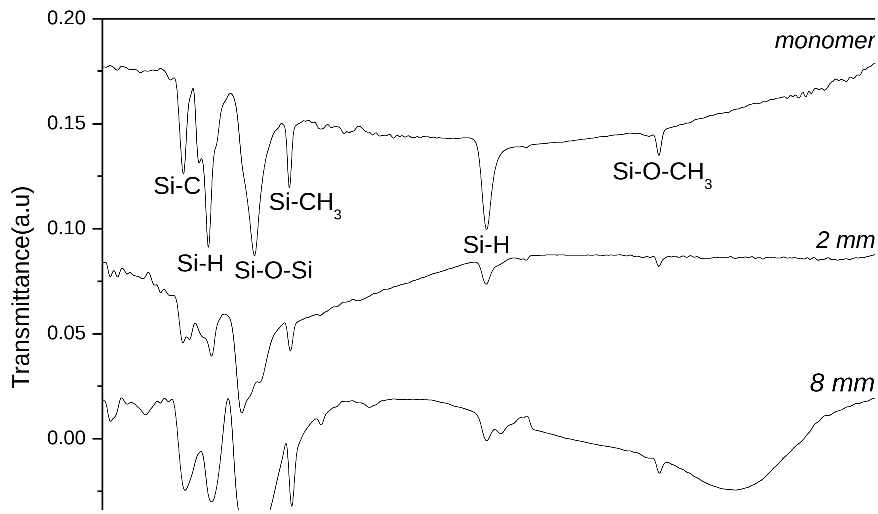

Figure 4: FTIR graph showing the retained chemistry of the monomer and the oxidised state of the coating deposited at the gap distances of 2 and 8 mm

Further FTIR analysis was carried out by integrating[16] the peak ratio of the Si-CH_3 to Si-O-Si functional groups at 1255 and 850 cm^{-1} respectively. It was observed that the Si-CH_3 to Si-O-Si ratio increased from 0.095 to 0.134 for the coatings deposited at 2 and 8 mm gap distance respectively. This 29% decrease in the Si-CH_3 to Si-O-Si ratio of the deposited coatings at 2 and 8 mm gap distances, is an indication of higher organic presence in the coating deposited at the lower gap distance. This again supporting the conclusion that the coatings at the 2 mm gap distance are less oxidised.

Coating refractive index was obtained using ellipsometry[27] operating at a wavelength of 632.8 nm. It was observed that the refractive index increased from 1.14 to 1.27 for the coatings deposited at 2 and 8 mm gap distances respectively. An increase in siloxane coating refractive index has previously been associated with a decrease in the organic fraction of the coating, again suggesting a higher level of coating oxidation.[27]

For the comparison trials on the effect of precursor chemistry on the mechanical durability of superhydrophobic coatings, in the case of the Tomcats coatings these were therefore deposited at a gap distance 2 mm and a precursor flow rate of 5 µl/min.

Superoleophilicity - The superhydrophobic Tomcats coating with a water contact angle of 155°, was tested for oil repellency by measuring the contact angle of decane[28] (surface tension γ 23.8 mN/m). Decane completely wetted the surface with contact angles <5°. The surface energy of the Tomcats coated sample is 5 mN m^{-1}. These kind of surfaces that possess both superhydrophobic (water contact angle >150°) and superoleophilic (oil contact angle <5°) properties may have a potential application in solvent or membrane separation of oil and water mixtures.[29] The HMDSO coating also exhibited superoleophilicity as decane completely wetted the surface.

Superhydrophobic Tomcats/Fluorosiloxane coating

Deposition studies were carried out with fluorosiloxane precursor at a flow rate of 5 µl min^{-1} and 2 mm gap distance. The resulting coatings however did not exhibit superhydrophobic properties. In this study the highest water contact angle achieved using a fluorosiloxane only precursor was 120°, although the coatings exhibited low surface energy of 6 mN m^{-1}, similar to that of HMDSO superhydrophobic coating. The addition of the fluorosiloxane to Tomcats was investigated as a means of enhancing the mechanical performance of the Tomcats SH coating. It is anticipated that the alkoxy functional group in the fluorosiloxane may increase cross-linking reactions within the mixture, and hence may yield a more mechanically robust polymer coating.[16] A mixture (50/50 vol/vol) of Tomcats and fluorosiloxane was nebulised into the plasma and deposited onto silicon wafer substrates at a 2 mm gap distance. The resulting Tomcats / fluorosiloxane coating mixture is given the abbreviation TCFS. Based on a series of TCFS deposition studies the following were the conditions which consistently yielded SH coatings: 7 µl min^{-1} precursor flow rate, 5 slm helium flow rate, 100 ml min^{-1} nitrogen flow rate and a gap distance of 2 mm.

FTIR analysis of the fluorosiloxane, Tomcats and TCFS coatings is given in Figure 5. The main peaks at 1270 cm^{-1} is attributed to the CF_2 functional group, while that at 785 cm^{-1} is ascribed to the CF_3 group. The absorption at 1100 cm^{-1} is assigned to the asymmetric Si-O-Si stretching.[26] These three functional groups are consistent with the linear chemical formula ($C_{14}H_{19}F_{13}O_3Si$) of the fluorosiloxane monomer, and demonstrate that the precursor chemistry is retained in the plasma deposited coating as reported previously.[16] It should be noted that the TCFS has peaks observed in the both the Tomcats and Fluorosiloxane precursors.

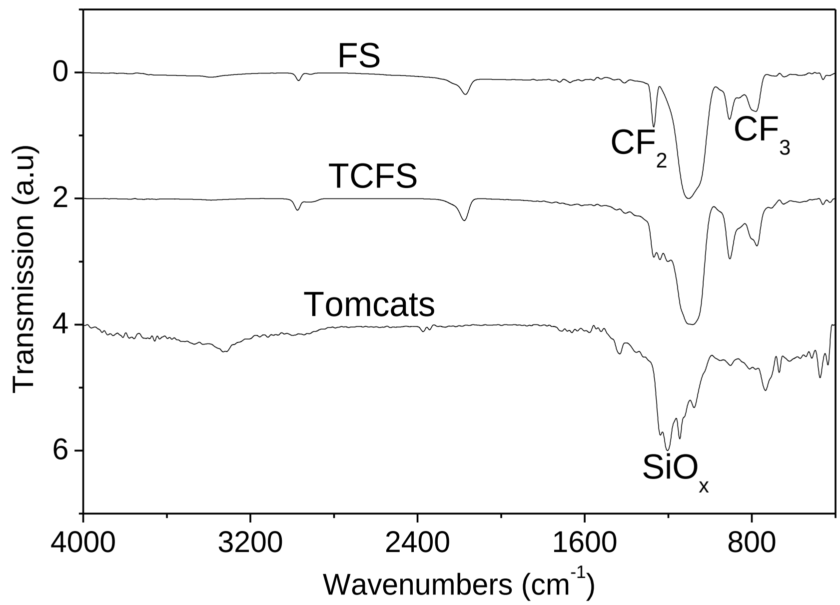

Figure 5: FTIR spectra of the Tomcats, fluorosiloxane (FS) and the TCFS coatings

The average water contact angle of the TCFS coated wafers was 158° and surface energy value of 3 mN m^{-1}. This contact angle was obtained with a 10 µl water droplet volume. It was attempted to also measure the contact angle with water volumes of 2 to 4 µl, which have been reported by other authors previously.[28] At these volumes the contact angle appeared to be considerably higher but the droplet simply slid off the surface making it impossible to obtain a consistent contact angle measurement. A comparison was made between the properties of the Tomcats and TCFS coatings both of which were deposited on silicon wafer substrates and also had similar thickness as detailed in Table 2.

Table 2: Comparison between the Tomcats and TCFS coatings

Coating type	Thickness (nm)	*Ra* (nm)	*Rq* (nm)	Water contact angle (°)
Tomcats	370	18	29	155
TCFS	352	13	17	158

While both coatings exhibit similar SH water contact angles, the roughness of the TCFS coating is considerably lower. This is demonstrated by the SEM and profilometry images given in Figure 6. A much higher level of particulates formation is observed in the case of the Tomcats coating.

These particulates are formed due to gas phase plasma reactions.[17] The reduced particulate formation in the case of the TCFS coating indicates that more polymerisation is taking place on the substrate surface than in the gas phase. A factor influencing the increase in the level of HMDSO precursor reaction in the plasma rather than at the substrate may be due to its lower flash point. The flash point of a liquid is that temperature as determined under experimental conditions, at which the liquid emits sufficient vapour to form a combustible mixture with air.[30] HMDSO precursor has a flash point of 0.6 °C while that of the Tomcats and fluorosiloxane precursors are 24 and 97 °C respectively.

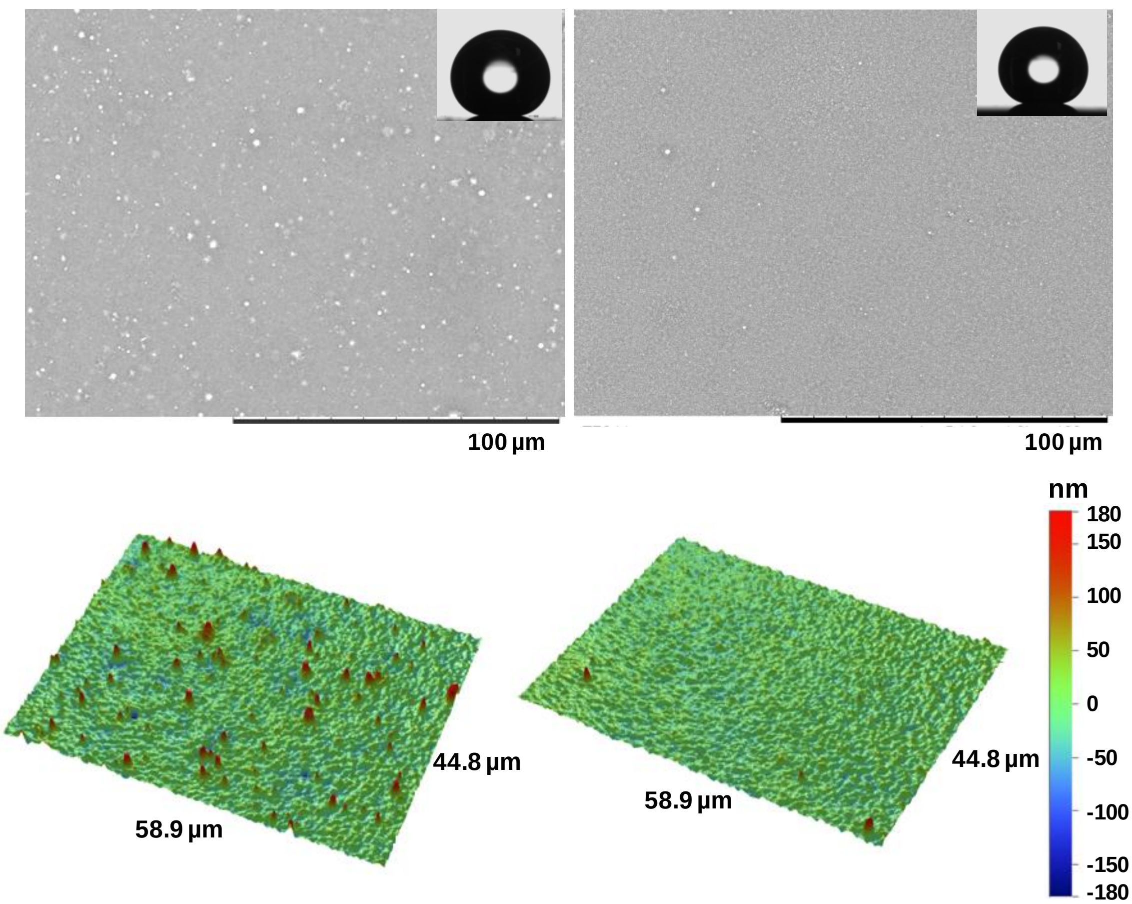

Figure 6: SEM (top) and Optical profilometry (down) images of the Tomcats (left) Ra 18 nm and TCFS (right) Ra 12 nm coated substrates. The images confirm the presence of numbers of particulates and lower surface roughness for the TCFS coating

XPS was used to calculate the stoichiometric elemental composition based on the chemical formula of Tomcats and TCFS (50/50 vol/vol mixture) monomer. The elemental composition of the plasma deposited Tomcats and TCFS coatings compared to these values are given in Table 3. The results demonstrate that a 6% reduction in the stoichiometric elemental composition (i.e. when compared with the Tomcats monomer) for carbon and silicon, while a 10% increase in the oxygen content was observed. The stoichiometric elemental composition for carbon in the TCFS coating reduced by 10% compared to the 1:1 TC:FS monomer mixture, while the oxygen and fluorine content increased by 3 and 8% respectively. No significant change was observed for the elemental composition of silicon. The observed decrease in the elemental composition of carbon and increase in oxygen in both coatings is due to coating oxidation which is to be expected in an atmospheric pressure helium plasma process.

Table 3: XPS comparison of the elemental composition of the precursor monomer and plasma deposited coating

Elements	**Tomcats**		**TCFS**	
	Monomer	**Coating**	**Monomer**	**Coating**
C (%)	33	27	41	31
O (%)	33	43	19	22
Si (%)	33	27	15	14
F (%)	-	-	26	32

XPS deconvolution of the C 1s curve for both coatings is shown in Figure 7. The curve fitting confirm that more cross-linking and polymerization reactions increased in the TCFS coating as anticipated, with the formation of new bonds (C-C=O) and (C-O), that were not present in the chemical formula of the mixture.

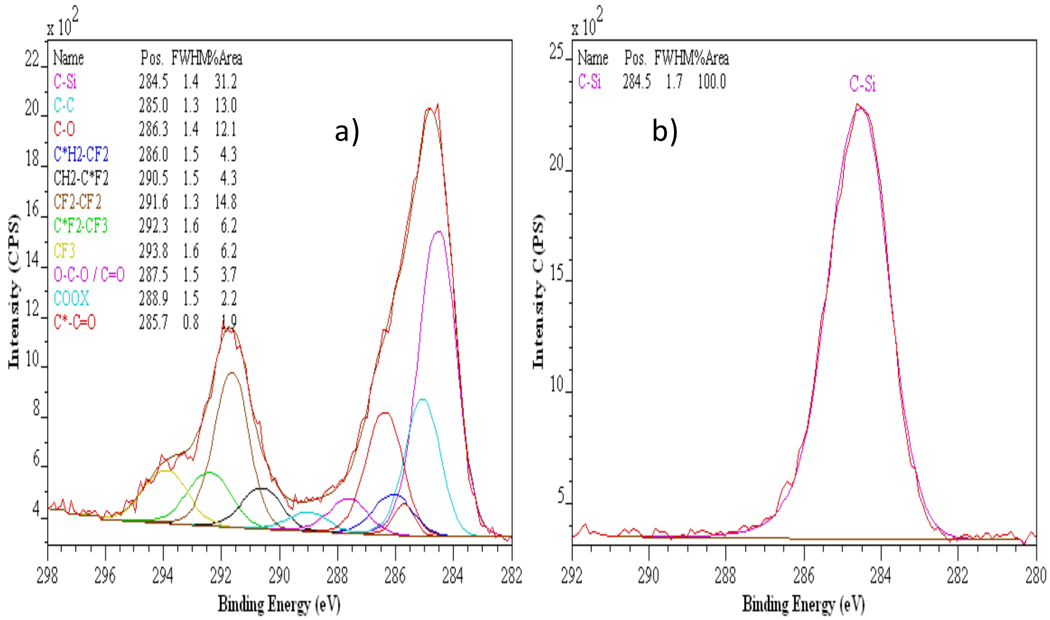

Figure 7: XPS C 1s curve fitting of the a) TCFS and b) Tomcats coating

Mechanical properties of the SH coatings

Nano scratch, nano tribometer and ultra indentation tests were carried on the HMDSO, Tomcats and TCFS coatings in order to assess their mechanical properties. The Nano Scratch test was used to compare the scratch resistance of the three SH coatings and their adhesion to the silicon wafer substrates. This Nano Scratch technique uses different sensors (such as force sensor and depth sensor) combined with an optical microscope to determine the critical loads. The minimum load at which adhesive failure occurs is called critical load (L_c) and is also known as adhesion strength, which is the stress required to remove a coating from the substrate.[31]

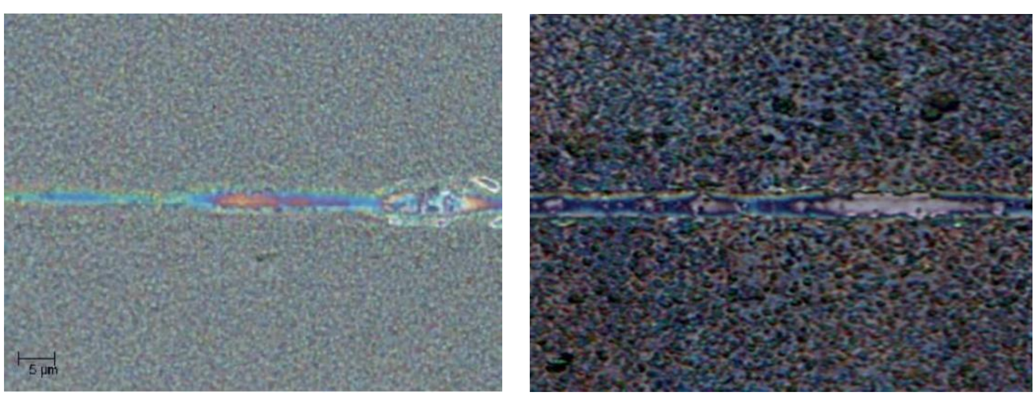

Figure 8: Image of first critical load (*Lc_1*) (left) and second critical load (*Lc_2*) (right) on the Tomcats SH coating. *Lc_1* is the normal load at which partial delamination appears on the film, while *Lc_2* is the normal load at which the full delamination of the film occurs

The first critical load (L_{C1}) is normally ascribed to the onset of failure, second critical load (L_{C2}) (see Figure 8) indicates film delamination.[32] It has been shown that L_C can be used to evaluate the performance of a DLC coating and its adhesion to the substrate.[33] A high L_C value would indicate good scratch resistance and adhesion to the substrate. The Lc_1 and Lc_2 values for the Tomcats, HMDSO and TCFS coatings are given in Table 4. It should be noted that the Lc_1 event did not occur for the TCFS coating. These results suggest that the adhesion of the TCFS coating to the substrate, and its scratch resistance is superior to that of the HMDSO and Tomcats coatings. Another important observation is that the scratch length at which Lc_2 occurred is 1.4 mm for the TCFS coating; however it is 0.5 and 0.4 mm for the HMDSO and Tomcats coatings respectively.

Table 4: Critical load, friction coefficient, Nano hardness (*H*) and Elastic modulus (*E*) of the coatings and the uncoated silicon wafer

Coatings	Thickness (nm)	L_{C1}, (mN)	L_{C2}, (mN)	*Friction coefficient*	H (MPa)	E (MPa)
Tomcats	370	3.2	15	0.38	19	785
HMDSO	350	8.1	21	0.52	8	313
TCFS	352	-	59	0.34	370	2500
Uncoated Si wafer	-	-	-	-	14398	167112

The coefficient of friction which is the ratio of the frictional force to the normal load was determined using Nano Tribometry.[34] A lower shear strength between the sliding ball and the coated surface would result in a lower friction force, and thus lower friction coefficient. It was observed that the TCFS coating has the lowest friction coefficient which at 0.34 is lower than that of the Tomcats and HMDSO coatings. The friction coefficient was almost constant in all cases during the test, which is an indication that the coating was not broken.

In order to determine the Nanoindentation hardness and elastic modulus, a matrix of 6 to 10 indentations were performed on the coated samples using the Ultra Nanoindentation tester. The Indentation Hardness (H_{IT}) and Elastic modulus (E_{IT}) of the coated and uncoated silicon wafer samples are given in Table 4. The results demonstrate that the hardness of the TCFS coating is 19 and 46 times higher than the Tomcats and HMDSO superhydrophobic coatings respectively. The elastic modulus of the TCFS coating is 3 and 8 fold higher than that of the Tomcats and HMDSO coatings. Some researchers have suggested that comparing the Hardness and Elastic modulus of polymers alone could be misleading as these properties could be largely influenced by variations in their microstructure, morphology, anisotropy, molecular weight and crosslink density.[20, 22] The resistance to plastic deformation (H^3/E^2) is reportedly preferred for evaluating the wear resistance of any material.[22, 32] The calculations suggest that the TCFS had the highest resistance to plastic deformation value of 8 in comparison to Tomcats and HMDSO coatings with values of 0.01 respectively. It has been reported that for a material with lower E/H ratio any contact with the material will more likely be elastic than plastic.[32] The E/H ratio 7 for the TCFS coating is considerably lower compared with the 41 and 39 for the Tomcats and HMDSO coatings respectively. This suggests that an elastic deformation mechanism is more likely to occur as the TCFS coating transmits an external force to the substrate, than the Tomcats and HMDSO coatings. This quality would be preferred in industrial applications as the deformation in the material would be reversible. These results indicate that the mechanical durability of the TCFS superhydrophobic coating has been enhanced probably due to increased plasma polymerisation and cross-linking reactions with the TCFS coating, which resulted in better coating adhesion to the substrate.

In order to verify and compare the results, similar tests were conducted on an uncoated silicon wafer substrate and the H^3/ E^2 calculation equates to 107, while E/H ratio is 12. This is to be expected as the uncoated silicon wafer substrate exhibits much higher hardness with better resistance to plastic deformation than the plasma polymerised coatings.

Abrasion test

These tests were carried out for the SH coated silicon wafer substrates using the ultrasonic probe immersed in the water / SiC powder mixture. The test results given in Figure 9 and Table 5 are the average obtained for 3 samples per test. All coatings exhibited a loss in superhydrophobic properties, but no coating was found to delaminate after the 150 minute abrasion treatment. The water contact angle of the TCFS coating decreased from 156 to 95° during the abrasion treatment (39%) reduction after the test period, in comparison to Tomcats 73% (154 to 41°) and HMDSO 56% (156 to 68°) coatings. These abrasion test results correlate with the Nano scratch test results detailed earlier.

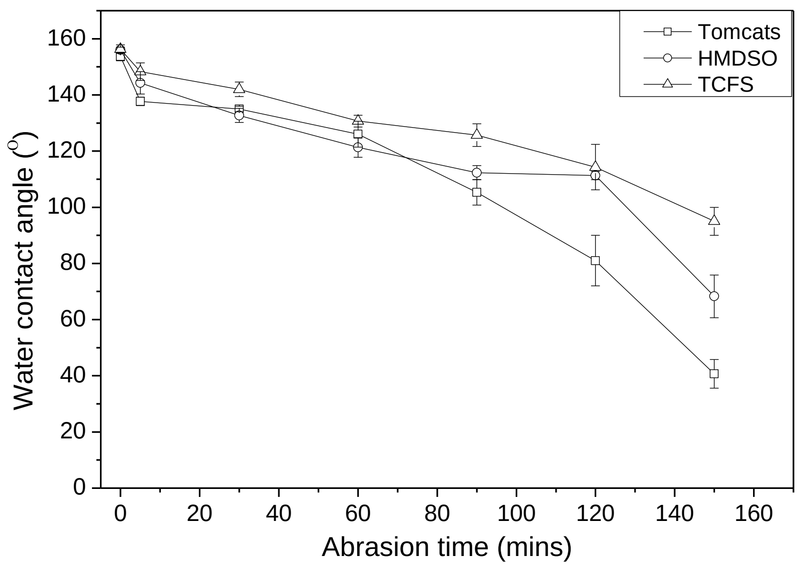

Figure 9: Abrasion tests for the Tomcats (thickness 370 nm), HMDSO (thickness 350 nm) and TCFS (352 nm) coatings after 150 minutes.

FTIR peak integration[16] of the Si-O and Si-CH_3 functional groups for the three coatings before and after the 150 mins abrasion treatment is presented in Table 5. The results confirm that the coatings survived the abrasion test with some slight reduction in the peak integration intensities, which is probably due to the wearing away and subsequent reduction in the coating thickness. Although this abrasion test should only be considered as qualitative rather than quantitative it was used to conclude that coating abrasion durability of the SH coatings is ranked as follows: TCFS > HMDSO > TC.

Table 5: FTIR peak integration of the Si-O and Si-CH_3 peaks of the coated samples after abrasion tests

Coatings	Si-O peak (a.u.)		Si-CH_3 peak (a.u.)	
	Before	***After***	***Before***	***After***
Tomcats	65 ± 3	45 ± 4	9 ± 0.3	6.1 ± 0.1
HMDSO	52 ± 3	41 ± 2	7 ± 0.1	5.5 ± 0.1
TCFS	58 ± 2	52 ± 2	7.8 ± 0.2	6.9 ± 0.1

XPS analysis was used to compare the siloxy chemistry of the three superhydrophobic coatings. The silicon Si 2p core level curve was fitted according to a methodology previously reported by O'Hare et al.[35] The simplified notation M [$(CH_3)_3SiO_{1/2}$], D [$(CH_3)_2SiO_{2/2}$], T [$(CH_3)SiO_{3/2}$] and Q [$SiO_{4/2}$] was used to represent the siloxy unit indicating the number of atoms attached to the silicon. A high Q-type siloxy chemistry would suggest increased oxidation whereas high M-type siloxy chemistry would indicate high organic content.

Table 6: XPS comparison of the siloxy chemistry in the SH coatings

Siloxy chemistry	Tomcats (%)	HMDSO (%)	TCFS (%)
M	0.6	3.1	0
D	35.9	37.7	0.9
T	43.2	33.4	67.5
Q	20.3	25.8	31.6

As demonstrated in Table 6, the TCFS coating was more oxidised with the highest Q-type siloxy chemistry than the Tomcats and HMDSO coatings. The enhanced mechanical performance of the TCFS as demonstrated earlier using Nano Scratch, Nanoindentation, Nano Tribology and Nano Abrasion tests may be associated with this higher level of Q-type and T-type siloxy chemistry. In a previous study by Twomey et al[36] comparing the mechanical behaviour of nm thick atmospheric plasma coatings, it was demonstrated that coatings with high Q-type siloxy chemistry after increased plasma exposure had better mechanical properties than their counterpart with lower Q-type chemistry. It should be noted that although the TCFS coating exhibited higher levels of oxidation with high Q-type and T-type siloxy chemistry, it also exhibits an increased inorganic character. It is anticipated that this would tend to increase the coating hydrophilicity. The superhydrophobic properties of TCFS are therefore associated with the presence of fluorine from the fluorosiloxane precursor.

A 2-D optical profile of the Tomcats, HMDSO and TCFS superhydrophobic coatings was obtained by scanning areas of 45 x 59 µm using the optical profilometry (Figure 10). The profiles of the coatings further demonstrate the needle-like profile observed in the 3-D scan of the HMDSO coating. The relative height of the 'needle' peaks is reduced in the case of the Tomcats and particularly that of the TCFS coatings. The enhanced durability observed in the TCFS coating may be partially associated with this reduction in needle peak height particularly when combined with enhanced levels of plasma polymerisation and cross-linking.

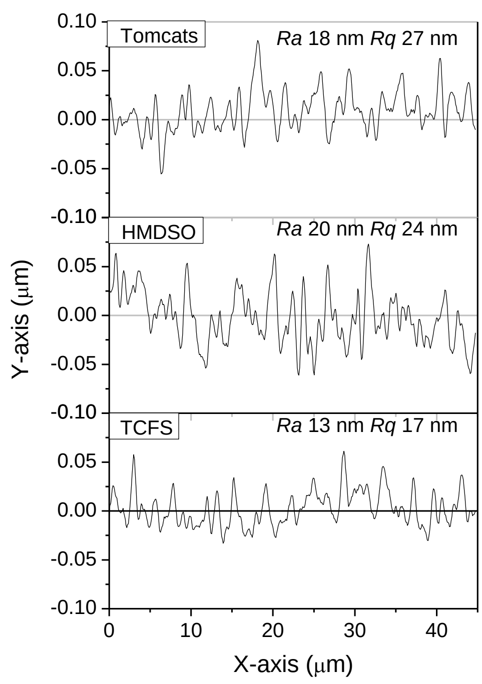

Figure 10: 2-dimensional optical profile of the SH Tomcats, HMDSO and TCFS coatings

Conclusion

Superhydrophobic coatings have been deposited using the PlasmaStream™ atmospheric plasma jet system using HMDSO, Tomcats and the mixture of Tomcats and fluorosiloxane (TCFS) precursors. The main focus of the research was to enhance the durability of the superhydrophobic coatings. This was successfully achieved through the deposition of the TCFS coating. XPS analysis demonstrated that this coating exhibited enhanced levels of cross-linking and polymerisation reaction compared with the Tomcats and HMDSO coatings. Nano Scratch, Nano Tribology and Ultra Nanoindentation tests also demonstrated that the TCFS coating also exhibited enhanced adhesion, hardness and wear resistance compared with these coatings. The abrasion resistance of the coatings was assessed using an ultrasonic jet abrasion technique and the abrasion performance correlate closely with the other tribological tests. In addition to enhance polymer cross-linking a factor influencing the enhanced wear and abrasion performance of the TCFS coating, is that its superhydrophobic properties are achieved with a reduction in the height of the 'needle-like' morphology, compared to the other coatings examined. It is concluded from this study that the superhydrophobic TCFS coating possess both superior mechanical properties and better abrasive wear resistance compared with that achieved with Tomcats and HMDSO coatings.

Acknowledgements

This work is supported by Science Foundation Ireland Grant 08/SRC11411

References

[1] Hoon Joo Lee and Stephen Michielsen 2007 Preparation of a superhydrophobic rough surface *Journal of Polymer Science Part B: Polymer Physics* **45** 253-61

[2] Genzer J and Efimenko K 2006 Recent developments in superhydrophobic surfaces and their relevance to marine fouling: a review *Biofouling* **22** 339-60

[3] Oner D and McCarthy T J 2000 Ultrahydrophobic Surfaces. Effects of Topography Length Scales on Wettability *Langmuir* **16** 7777-82

[4] Onda T, Shibuichi S, Satoh N and Tsujii K 1996 Super-water-repellent fractal surfaces *Langmuir* **12** 2125-7

[5] Milella A, Mundo R D, Palumbo F, Favia P, Fracassi F and d'Agostino R 2009 Plasma Nanostructuring of Polymers: Different Routes to Superhydrophobicity *Plasma Processes and Polymers* **6** 460-6

[6] Erbil H 2003 Transformation of a simple plastic into a superhydrophobic surface *Science* **299** 1377

[7] Tadanaga K, Katata N and Minami T 1997 Formation process of super-water-repellent Al sub 2 O sub 3 coating films with high transparency by the sol-gel method *Journal of the American Ceramic Society(USA)* **80** 3213-6

[8] Li M, Zhai J, Liu H, Song Y, Jiang L and Zhu D 2003 Electrochemical Deposition of Conductive Superhydrophobic Zinc Oxide Thin Films *The Journal of Physical Chemistry B* **107** 9954-7

[9] O'Neill L, Herbert A P F, Stallard C and Dowling D P 2010 Investigation of the Effects of Gas versus Liquid Deposition in an Aerosol Assisted Corona Deposition Process *Plasma Processes and Polymers* **7** 43-50

[10] Yang S, Liu C, Su C and Chen H 2009 Atmospheric-pressure plasma deposition of SiOx films for super-hydrophobic application *Thin Solid Films* **517** 5284-7

[11] Ji Y-Y, Kim S-S, Kwon O P and Lee S-H 2009 Easy fabrication of large-size superhydrophobic surfaces by atmospheric pressure plasma polymerization with non-polar aromatic hydrocarbon in an in-line process *Applied Surface Science* **255** 4575-8

[12] Kim S H, Kim J-H, Kang B-K and Uhm H S 2005 Superhydrophobic CFx Coating via In-Line Atmospheric RF Plasma of He-CF_4-H_2 *Langmuir* **21** 12213-7

[13] Chen G, Chen S, Feng W, Chen W and Yang S-z 2008 Surface modification of the nanoparticles by an atmospheric room-temperature plasma fluidized bed *Applied Surface Science* **254** 3915-20

[14] Woodward I, Schofield W C E, Roucoules V and Badyal J P S 2003 Super-hydrophobic Surfaces Produced by Plasma Fluorination of Polybutadiene Films *Langmuir* **19** 3432-8

[15] Albaugh J, O'Sullivan C and O'Neill L 2008 Controlling deposition rates in an atmospheric pressure plasma system *Surface and Coatings Technology* **203** 844-7

[16] Nwankire C E, Ardhaoui M and Dowling D P 2009 The effect of plasma polymerised Si-H rich polymethylhydrogen siloxane (PHMS) on the adhesion of silicone elastomers *Polymer International* **58** 996-1001

[17] Dowling D P, Ramamoorthy A, Rahman M, Mooney D A and MacElroy J M D 2009 Influence of Atmospheric plasma source and Gas composition on the properties of deposited siloxane coatings *Plasma Processes and Polymers* **6** S483-S9

[18] Owens D K and Wendt R C 1969 Estimation of the surface free energy of polymers *Journal of Applied Polymer Science* **13** 1741-7

[19] Steinmann P, Tardy Y and Hintermann H 1987 Adhesion testing by the scratch test method: the influence of intrinsic and extrinsic parameters on the critical load *Thin Solid Films* **154** 333-49

[20] VanLandingham M, Villarrubia J, Guthrie W and Meyers G 2001 Nanoindentation of polymers: An overview *Macromolecular symposia* **167** 15-44

[21] Doerner M and Nix W 1986 A method for interpreting the data from depth-sensing indentation instruments *J. Mater. Res* **1** 601-9

[22] Leyland A and Matthews A 2000 On the significance of the H/E ratio in wear control: a nanocomposite coating approach to optimised tribological behaviour *Wear* **246** 1-11

[23] Xiu Y, Liu Y, Hess D W and Wong C P 2010 Mechanically robust superhydrophobicity on hierarchically structured Si surfaces *Nanotechnology* **21** 155705

[24] Twomey B, Dowling D, Byrne G, O'Neill L and O'Hare L-A 2007 Properties of siloxane coatings deposited in a reel-to-reel atmospheric pressure plasma system *Plasma Processes and Polymers* **4** S450-S4

[25] O'Neill L and O'Sullivan C 2009 Polymeric Coatings Deposited From an Aerosol-Assisted Non-thermal Plasma Jet *Chemical Vapor Deposition* **15**

[26] Colthup N B, Daly L H and Wiberley S E 1975 *Introduction to infrared and Raman spectroscopy* (New York: Academic Press)

[27] Twomey B, Rahman M, Byrne G, Hynes A, O'Hare L-A, O'Neill L and Dowling D P 2008 Effect of plasma exposure on the chemistry and morphology of aerosol-assisted, plasma-deposited coatings *Plasma Processes and Polymers* **5** 737-44

[28] Tuteja A, Choi W, Ma M, Mabry J M, Mazzella S A, Rutledge G C, McKinley G H and Cohen R E 2007 Designing Superoleophobic Surfaces *Science* **318** 1618-22

[29] Feng L, Zhang Z, Mai Z, Ma Y, Liu B, Jiang L and Zhu D 2004 A super-hydrophobic and super-oleophilic coating mesh film for the separation of oil and water *Angewandte Chemie* **116** 2046-8

[30] Liaw H-J and Chiu Y-Y 2003 The prediction of the flash point for binary aqueous-organic solutions *Journal of Hazardous Materials* **101** 83-106

[31] Park H and Kwon D 1997 An energy approach to quantification of adhesion strength from critical loads in scratch tests *Thin Solid Films* **307** 156-62

[32] Shtansky D V, Gloushankova N A, Bashkova I A, Petrzhik M I, Sheveiko A N, Kiryukhantsev-Korneev F V, Reshetov I V, Grigoryan A S and Levashov E A 2006 Multifunctional biocompatible nanostructured coatings for load-bearing implants *Surface and Coatings Technology* **201** 4111-8

[33] Ramírez G, Tarrés E, Casas B, Valls I, Martínez R and Llanes L 2009 Contact Fatigue Behavior of PVD-Coated Steel *Plasma Processes and Polymers* **6** S588-S91

[34] Bhushan B, Israelachvili J and Landman U 1995 Nanotribology: friction, wear and lubrication at the atomic scale *Nature* **374** 607-16

[35] O'Hare L-A, Parbhoo B and Stuart R. Leadley 2004 Development of a methodology for XPS curve-fitting of the Si 2p core level of siloxane materials *J. Surf. Interface Anal.* **36** 1427-34

[36] Twomey B, Byrne G, Hynes A, O'Neill L and Dowling D 2009 Evaluation of the mechanical behaviour of nanometre-thick coatings deposited using an atmospheric pressure plasma system *Surface and Coatings Technology* **203** 2021-9